ISSN: 0976 – 2965
IJBET (2017), 6(3):18-31

Application of Titanium Dioxide-Graphene Nanocomposite Material in Visible Light Radiation for Photocatalytic Degradation of Water Pollutants

Farid Abu Shammala[1] and Kelvin O'Halloran[2]
1 Faculty of Engineering, University of Palestine , El-Zahra City, Gaza, Palestine
2 Scientific Services and Data Systems, Seqwater, 117 Brisbane St., Ipswich, Queensland 4305, Australia
drfaridshammala@hotmail.com

ABSTRACT

The water pollutant compounds were photocatalytically remediated from water using graphene oxide (GEO)-titanium oxide (TiO_2) nanocomposite material in visible light radiation. The GEO -TiO_2 nanocomposite was synthesized using sol-gel technique, and its structural & morphological properties were studied using scanning electron microscopy (SEM), X-ray diffraction (XRD), transmission electron microscopy (TEM), particle analyzer based techniques, Raman spectroscopy, FTIR spectroscopy, fluorescence emission spectroscopy and UV-Visible spectroscopy. Thus, this research reports the photocatalytic effectiveness of GEO-TiO2 nanocomposite material in the degradation of four petroleum-based chemicals (2, 4-dihydroxybenzoic acid, 4-chlorophenol, Toluene and naphthalene), under the conditions defined in this research. 96% of 2, 4-dihydroxybenzoic acid, 94% of 4-chlorophenol, 90% of toluene, only 40% of naphthalene remediation from the contamination water for exposure of only 2 hour of visible light, without using surfactant. And 98% of 2, 4-dihydroxybenzoic acid, 95% of 4-chlorophenol, 92% of toluene, only 55% of naphthalene remediation from the contamination water for exposure of only 2 hour of visible light, with using surfactant. Moreover, 99.5% of 2, 4-dihydroxybenzoic acid, 98.8% of 4-chlorophenol, 98.5% of toluene, 96% of naphthalene have been remediated using GEO-TiO2 nanomaterial under UV light. The degradation of water pollutants was monitored by UV-Vis spectroscopy and high performance liquid chromatography (HPLC). Thus, photocatalytic activity to remove organic pollutants from water employing GEO-TiO2 nanocomposite without doping is successfully showed, and therefore, a new gate in research for these materials is opened.

Keywords: GEO -TiO2, photocatalyst, decontamination, 2, 4-dihydroxybenzoic acid, 4-chlorophenol, Toluene, Naphthalene

INTRODUCTION

Global warming and the increment of pollutant concentrations are just two of the environmental issues associated with societal development. From the past few decades the rampant use of industrial chemicals a large amount of pollutants are disposed continuously into water bodies, which lead to undesirable accumulation of toxic components leading to serious environmental and health problems [1]. Therefore, it is advisable to look for an economical and feasible technique for remediation of such hazardous environmental effluents [2]. Advanced oxidation processes (AOPs) have been proved as an excellent method for the degradation of environmentally hazardous material [1]. Photocatalysis is the advanced oxidation processes and received much more attention for the degradation of pollutants in aqueous phase by simple and efficient manner [3]. One possible way to address those and other existing environmental problems could be through the development of highly-efficient photocatalysts; exploiting processes that are based in solar energy. Semiconductor-based photocatalysis relies on the active absorption of a photon from a semiconductor to create an electron-hole pair. This process depends on the band gap of the material [4]. Then, the excited electron has to be separated from the hole created to avoid recombination. This can be used to generate an ultrafast photocurrent response [5]. The electron can also be used to reduce chemicals in the environment by generating radical species such as hydroxyl radicals; which can initiate, for example, degradation reactions [6].

Research on carbon-based photocatalytic nanomaterials has been a field in continuous expansion in the last years. Graphene (or its derivatives) is currently one of the most studied materials due to its high surface area, photodegradation resistance, optical transparency and high charge mobility values. All of these

excellent properties are highlighted for applications in various research areas. The incorporation of small amounts of reduced graphene oxide (RGO) sheets in semiconductors matrices is also a strategy widely used to improve the physicochemical properties, which cannot normally be achieved using conventional composites or pristine semiconductors.

For a semiconductor to be considered a good photocatalyst, the compound must be photoactive, it must have different electron and hole processes so they do not recombine, it must be able to absorb UV and visible radiation effectively, be photo-stable and be biologically and chemically inert, with the exception of the reaction that it has to catalyze. Besides, in order to be mass-produced, it has to be easy to fabricate, cost effective and non-toxic. Some of the most adequate and traditionally studied semiconductors are TiO_2, ZnO, CdS, ZnS and Fe_2O_3 [7]. Nevertheless, those materials have some limitations (e.g., TiO_2 has a limited photoactivity with the radiation provided by solar light that can be potentially overcome by the use of graphene and its derivatives.

Up to date, much efforts have been carried out to extend the spectral response of photocatalyst into UV region for photodegradation of pollutants in various ways, including doping with metals, nonmetals, rare earth metals and coupling with other semiconductor [8]. Doping of TiO_2 with transition and rare earth metal have received much attention for improving the photocatalytic activity due to vacant d and f orbitals. Among various transition metal ions, Mn^{2+} received more attention than other transition metal ion due to similarity in ionic radii of Mn^{2+} and Ti^{4+}.

Heterogeneous semiconductor photocatalysts have received significant attention owing to their potential application in a wide range of photoinduced reactions, notably photocatalytic hydrogen production, removal of organic contaminants and air pollutants, and electricity production using solar cells [9]. Nanoscaled TiO_2 photocatalyst has attracted much more attention due to its stable chemical and physical property, lower cost and excellent photocatalytic performance [10-12]. However, the broad bandgap of TiO_2 seriously restrains its practical application in the area of full-wavelength of solar spectrum. Recently, graphene (GR) is used as an ideal supporter to load with TiO_2 nanoparticles, due to the excellent conductive properties, mechanical properties and chemical stability [13-17]. Although the TiO_2-graphene has become a new photocatalyst with efficient photoactivity, there are also some problems on this novel photocatalytic composites, such as the origin of its visible light response [18]. And another problem is the choosing of the appropriate reductant using for the reduction of GO.

Herein, we developed and optimized GEO-TiO_2 nanoparticles synthesis process for obtaining the large surface area and 2, 4-dihydroxybenzoic acid, 4-chlorophenol, toluene and naphthalene based organics in water were remediated in visible light. The GEO-TiO_2 nanoparticles were synthesized using sol-gel technique, and studied. G-TiO_2 nanoparticles were characterized by XRD, SEM, TEM, Raman spectroscopy, FTIR spectroscopy, particle analyzer based techniques, fluorescence spectroscopy and UV-vis spectroscopy. Thus, it is important to verify the photocatalytic activity of these unmodified carbon materials for the removal of organic compounds in water. GEO-TO_2 has attracted great interest to us because of its easy availability in bulk quantities, readiness for functionalization by chemical reaction, good dispersion in water and high biocompatibility [19]. Thus, this research shows for the first time the capacity of titanium dioxide-graphene nanocomposite material to remove organic pollutants from aqueous solutions under visible light radiation.

METHODS

Materials

Graphite (Electron Microscopy Sciences, No. 70230), distilled water (J.T. Baker), 4-chlorophenol (≥99% Sigma Aldrich), Sulfuric acid (H_2SO_4, Baker, 98%), potassium permanganate ($KMnO_4$, Merck), hydrogen peroxide (H_2O_2, Baker, 30%) and distilled water (H_2O) were used as received. Graphene oxide (GEO) were synthesized from graphite by a methodology reported in a previous work [20], and described briefly below.

Synthesis of graphene oxides-TiO2 Nanocomposite

The synthesis of GEO-TiO2 nanocomposite materials showed better yield through a sol-gel synthesis process [21]. First, H_2SO_4 (46 mL) was added into the reaction flask maintained at 0°C (±2°C) (ice bath), then graphite (2 g) and $KMnO_4$ (6 g) were added slowly. After an increase in temperature to 35°C (±2°C), the mixture was stirred by a magnetic stirring bar and mixed for 2 h. Later, the excess water was incorporated to the

mixture and H_2O_2 (10 ml) was added until there was no gas production. Then, filtration was performed with distilled water in a glass filter, and the obtained brown GO was dried in an oven (Barnstead Thermoline, Model 3478) at 65°C for 12 h. After that, a solution containing 100 mg of dried GEO in 10 mL of H_2O was prepared. The synthesis of nanocomposite GEO-TiO2 was initiated by using a mixture of titanium (IV) isopropoxide in propanol solution. Initially, 1.93 gram (g) of graphene was mixed with 200 ml of propanol with an addition of 40 mL of titanium (IV) isopropoxide, and left on stirring for 30 minutes. HCl was added drop wise and the solution was left stirring for 24 hours at room temperature. This solution was sonicated for 3 h at room temperature with the assistance of an ultrasonic bath (Branson 1510R-MTH) at 55 degassing units, in order to obtain graphene oxide sheets (GEO). The precipitate formed after 24 h of reaction under stirring was washed in deionized water for removal of any unreacted organic residues by centrifugation process. The centrifuged G-TiO2 nanoparticles were dried at 100˚C for 24 h.

Adsorption test

The organic contaminants (2, 4-dihydroxybenzoic acid, 4-chlorophenol, Toluene and naphthalene) at different concentrations were used to decontaminate using GEO-TiO2 nanocomposite photocatalyst. A 100 W lamp was employed to simulate the solar light intensity of 800 - 1000 W/m2. The contaminants solution of G-TiO2 were stirred in closed glass container, and kept closed during the completion of the experiment. Samples were collected at regular intervals, and centrifuged to separate composite GEO-TiO2 particles from measuring solution. The centrifuged sample of 1 µL solution was passed through a gas chromatography. Diesel, toluene and naphthalene containing water samples have been kept in the identical conditions, and decontaminated water samples have been collected as a function of time using GEO-TiO2 photocatalyst. These pollutants may get evaporated especially under stirring and light exposure conditions. It is useful to add a control experiment using the same equipment setup while changing the GEO-TiO2 to pure TiO2. The retention time (in min) vs. area under curve was plotted to understand each organic contaminant in the water sample. The ratio of concentrations as Co (initial concentration) and Cn (concentration of solution at different timed samples with % of sample remained in the solution) were used to understand the change in percentage of concentration with the use of GEO-TiO2 nanocomposite photocatalyst [21]. Adsorption test consisted on placing an aqueous solution of 2, 4-dihydroxybenzoic acid, 4-chlorophenol, Toluene and naphthalene with a concentration of 30 ppm and neutral pH into a tubular glass reactor, adding graphene oxide (0.8 g/L) with magnetic stirring (1000 rpm) and then, the reactor was covered with aluminium foil to prevent contact with external light. The reaction time was 100 minutes and aliquots were taken at 20, 40, 60, 80 and 100 minutes.

Photocatalyst test

For these experiments, 30 mL of 2, 4-dihydroxybenzoic acid, 4-chlorophenol, Toluene and naphthalene (30 ppm) at neutral pH were placed in the same reactor used for the adsorption test and induced with UV irradiation from a lamp (Pencil UV lamp, 254 nm, 5.5 W). Light source was located in the centre of the vessel along with a magnetic stirrer (1000 rpm). The reactor temperature was maintained at 24°C +/- 2°C and the reactor was covered with aluminium foil to prevent contact with external light. The reaction time was 100 minutes and aliquots were taken after 20, 40, 60, 80 and 100 minutes. The photocatalytic efficiencies of GEO were determined in the same tubular glass reactor used for the photolysis test with the same continuous stirring (1000 rpm). The total reaction volume was 30 ml. The tests were performed using 0.8 g/L of graphite and graphene oxides, with 30 ppm of 2, 4-dihydroxybenzoic acid, 4-chlorophenol, Toluene and naphthalene at neutral pH. The reactor temperature was maintained at 24°C +/- 2°C and aluminium foil was placed around the reactor. The reaction time was 100 minutes and aliquots were taken after 20, 40, 60, 80 and 100 minutes.

Characterization

Powder X-ray diffraction (XRD) was used for phase identification and to estimate the crystallite size of the anatase nanoparticles. The XRD spectra were obtained at room temperature with a Siemens X-ray diffractometer (Model: B5005) using Cu K radiation (Å), and data were collected from 2 = 20˚ to 80˚ at a step size of 0.020˚/s. FTIR spectra of TiO_2, GEO, and TiO_2-graphene oxide were obtained via a Varian 3100 FT-IR spectrophotometer using KBr pellets. Transmission electron microscopy (TEM) images and selected area electron diffraction (SAED) of the synthesized composite were performed via a JEOL JEM 3010 electron microscope to observe the surface morphology of the TiO_2-GEO composite.

ISSN: 0976 – 2965
IJBET (2017), 6(3):18-31

EDX analysis was recorded on a JEOL JED-2300 scanning electron microscope to identify the elemental composition. Fourier transform infrared spectroscopy (FT-IR) of GEO samples was performed with a scanning range of 4000-500 cm^{-1} with resolution of 1 cm^{-1}. Raman spectroscopy of the carbon samples was carried on a Micro-Raman (Dilor, Lab Ram), with measurements at 488 nm incident laser light with a spectral resolution of 1 cm^{-1}. UV-vis spectroscopy was carried out on a HACH DR5000 spectrophotometer at wavelengths of 200–1100 nm to determine the absorption bands characteristic of the pollutants solution and monitor the progress of pollutants removal from the solution by adsorption, photolysis and the photocatalytic processes. HPLC (High Performance Liquid Chromatography) was performed with a mobile phase of H_2O with 5 mmol H_2SO_4 and methanol (80:20), a flow rate of 1 mL/min and an Ascentis Express C_{18} 3 cm × 4.6 mm (2.7 µm) SUPELCO column for the determination of intermediate compounds. The charge recombinations of TiO_2-GEO and TiO_2 were compared by obtaining the fluorescence emission spectra. Fluorescence spectroscopy analysis was carried out at room temperature via a Perkin Elmer Luminescence spectrometer (LS 55) equipped with a powder holder accessory, and the excitation wavelength was set at 300 nm.

RESULTS AND DISCUSSION

The aforementioned photoelectrochemical properties of optimized GEO-TiO_2 nanoparticles prepared in our laboratory can be used to develop enhanced photovoltaic systems, have lead to produce novel materials to be incorporated and improve existing applications, such as organic pollutant decompositors. Herein, we have presented a facile route for the in situ preparation of GEO-TiO_2 nanocomposites having excellent photocatalytic activity. TiO_2 nanoparticles is incorporated into graphene oxide sheets, and the resultant mixture is solvothermally treated to attain TiO_2-reduced graphene oxide nanocomposites without the use of any additional reducing agents. The well alignment of the TiO_2 nanoparticles over individual graphene oxide layers was confirmed using various characterization techniques, such as scanning electron microscopy (SEM), X-ray diffraction (XRD), transmission electron microscopy (TEM), particle analyzer based techniques, Raman spectroscopy, FTIR spectroscopy, fluorescence emission spectroscopy and UV-Visible spectroscopy.

SEM and TEM Study

Both transmission electron microscope (TEM) and scanning electron microscope (SEM) and were utilized to characterize the morphologies of GEO-TiO_2 nanocomposites. Figure 1 exhibits TEM picture of the TiO_2-reduced graphene oxide nanocomposite at different magnifications. The Figure 1(a) observed the particle size of 20 - 50 nm for GEO-TiO_2 nanoparticle. Further, magnification in Figure 1(b) and Figure 1(c) reveals well-defined graphene coated TiO_2 nanoparticles. Figure 2 (a) shows a typical SEM image of the GEO-TiO_2, which was pretty tidy without any contaminant on their surface. The nanocomposite structure was observed to be bunches of nanocomposite with several microns long, but the width varies from about 20 nm up to 200 nm, namely nanosheets. Further sonication will break down these nanosheets into single nanocomposite with diameter of about 20 nm as shown in Figure 1 (d). We also used the hydrothermal method to reduce GEO without adding TiO_2 nanostructures for control experiment, and the TEM image of GEO-TiO_2 structure in Fig. 2 (d) demonstrates that this reduction process with ethanol as the reductive agent is effective to produce graphene sheets with thin layers. After a second hydrothermal process, the representative TEM images of GEO-TiO_2 nanocomposite structure with different magnifications were shown in Figure 2 (b) and (c), which presented a uniform covering of TiO_2 nanoparticles over grapheme oxide sheets. By comparing Figure 2 (b) with (a), it is noticed that the wide TiO_2 nanosheets decomposed into very thin nanocomposite that cover GEO surface in a reasonable uniform fashion. The SEM image of as-synthesized GEO-TiO_2 nanostructure was shown in Fig. 2 (c), which suggests that the dense TiO_2 attachment was scattered over throughout the graphene sheets on both sides, attached on the ridges and wrinkles of GEO to form agglomeration, indicating that TiO_2 is easier to form Ti-O-C bond with GEO at the locations of defects, including functional groups.

ISSN: 0976 – 2965
IJBET (2017), 6(3):18-31

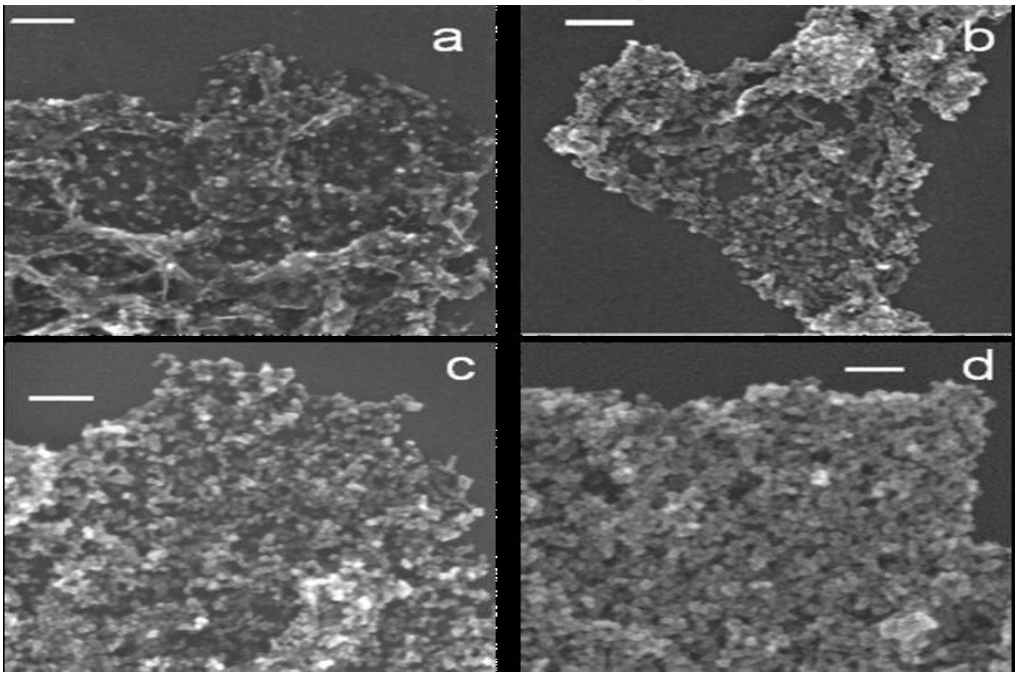

Figure 1. Transmission electron microscope (TEM) pictures of GEO-TiO_2 nanocomposite at different magnification (a)-(d).

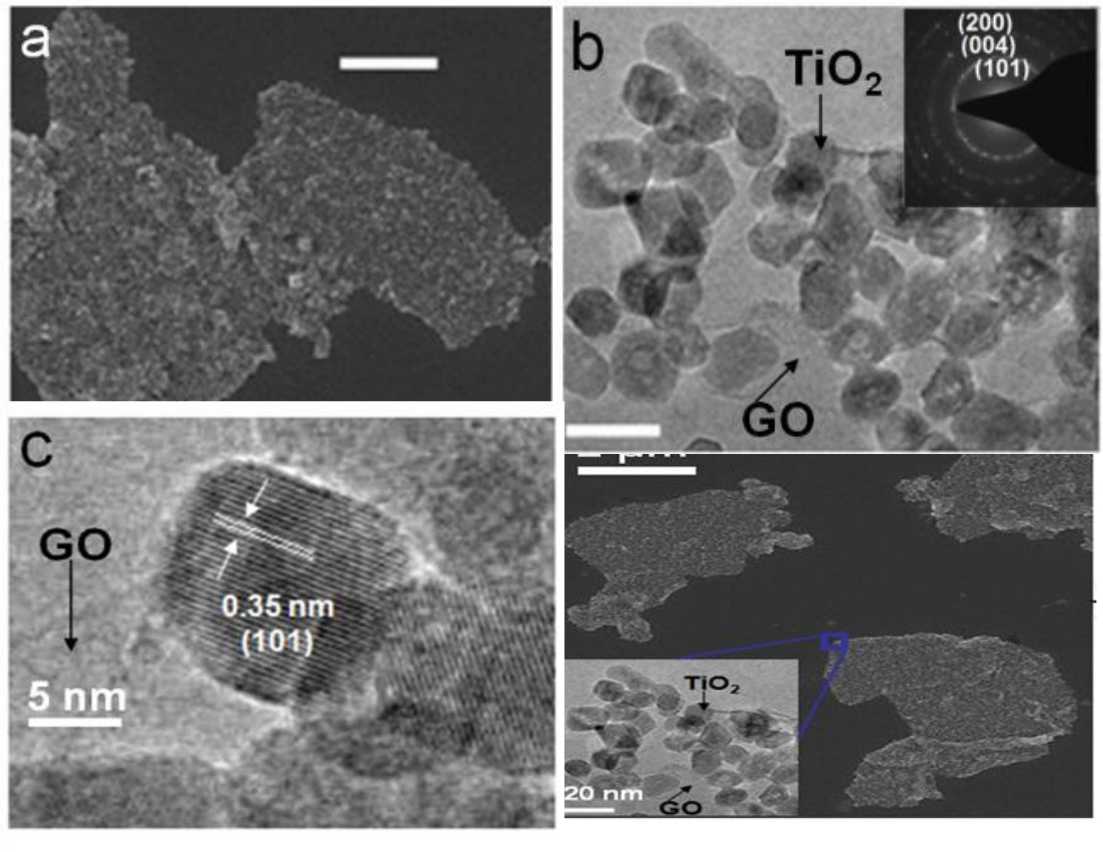

Figure 2. Scanning electron microscope (SEM) images of GEO-TiO_2 nanocomposite at different magnifications (a)-(d). (a) SEM image with scale bar of 400 nm, (b) low magnification with scale bar of 20 nm and (c) high magnification TEM images of TiO_2 nanocrystals grown on graphene oxide sheets.

ISSN: 0976 – 2965
IJBET (2017), 6(3):18-31

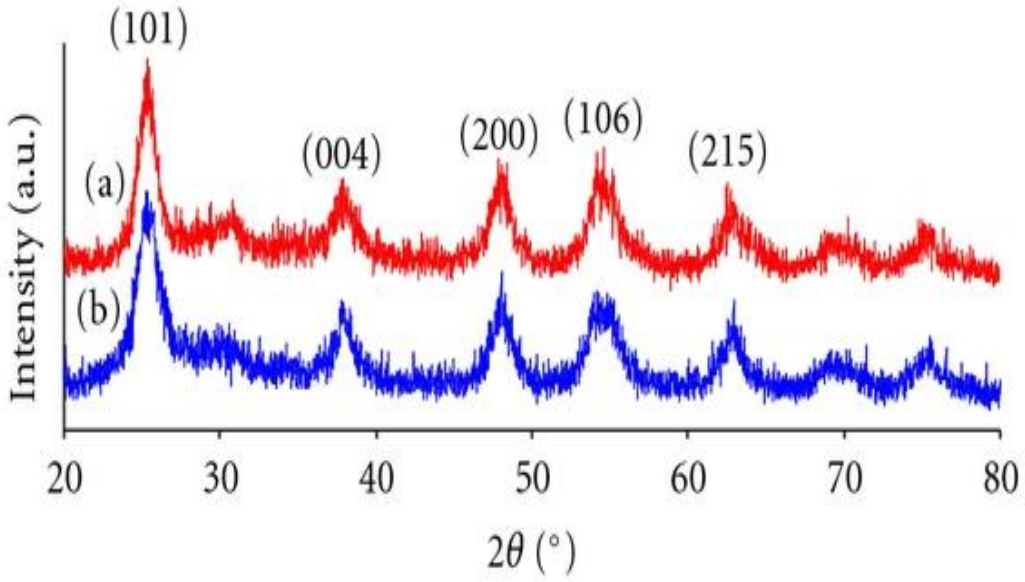

Figure 3. XRD image of two G-TiO_2 nanocomposite annealed at different time.

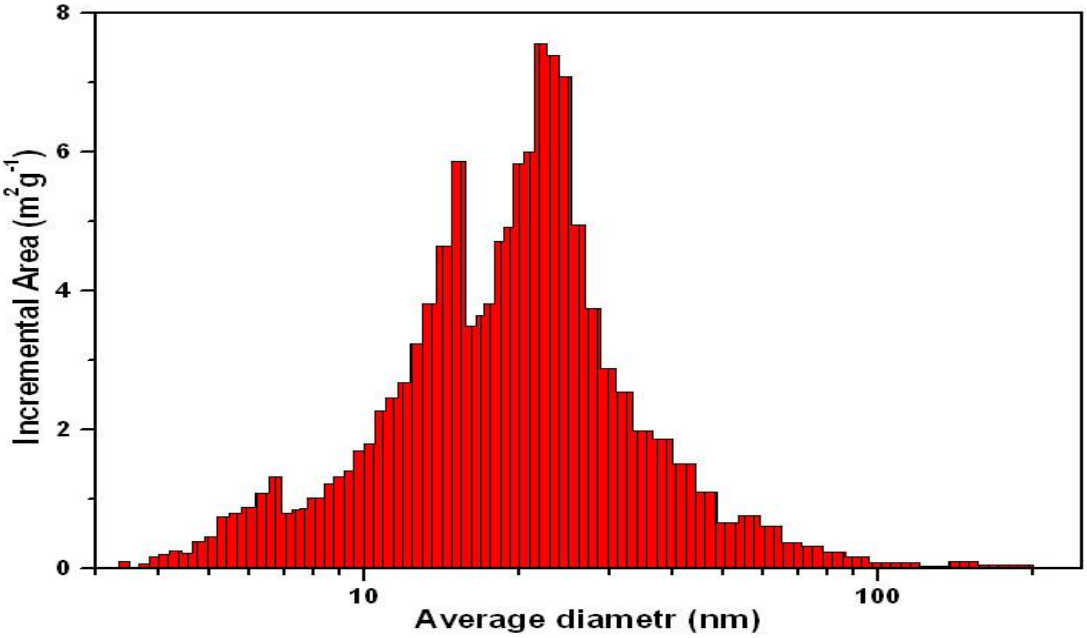

Figure 4. The particle distribution of GEO-TiO_2 nanocomposite in water.

ISSN: 0976 – 2965
IJBET (2017), 6(3):18-31

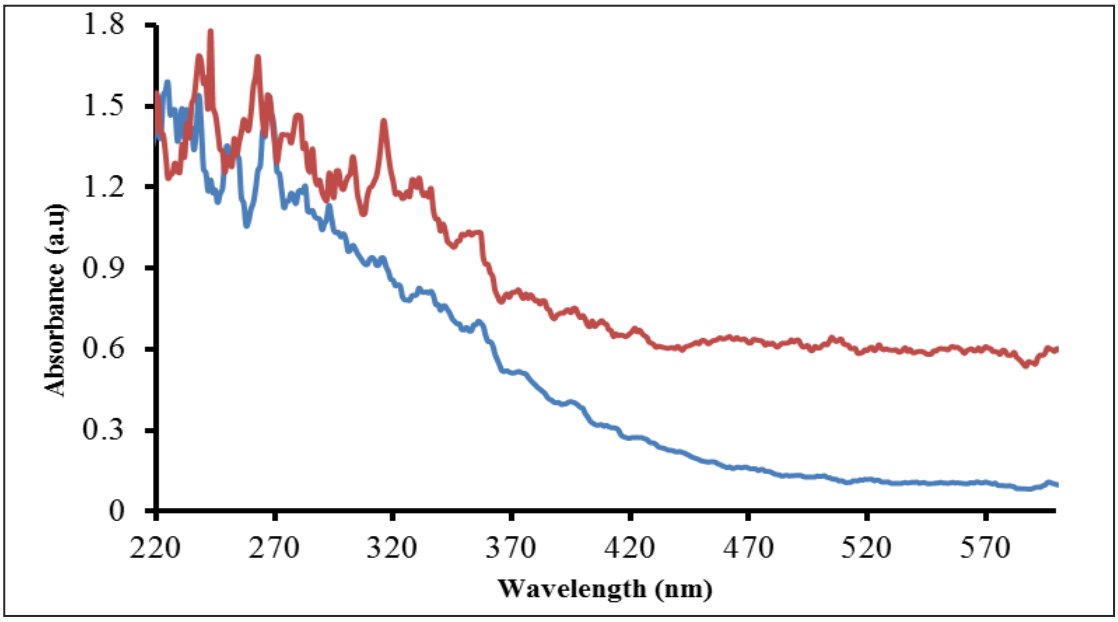

Figure 5. UV-visible absorption spectra of TiO2 particles (blue) and GEO-TiO_2 nanocomposites (red).

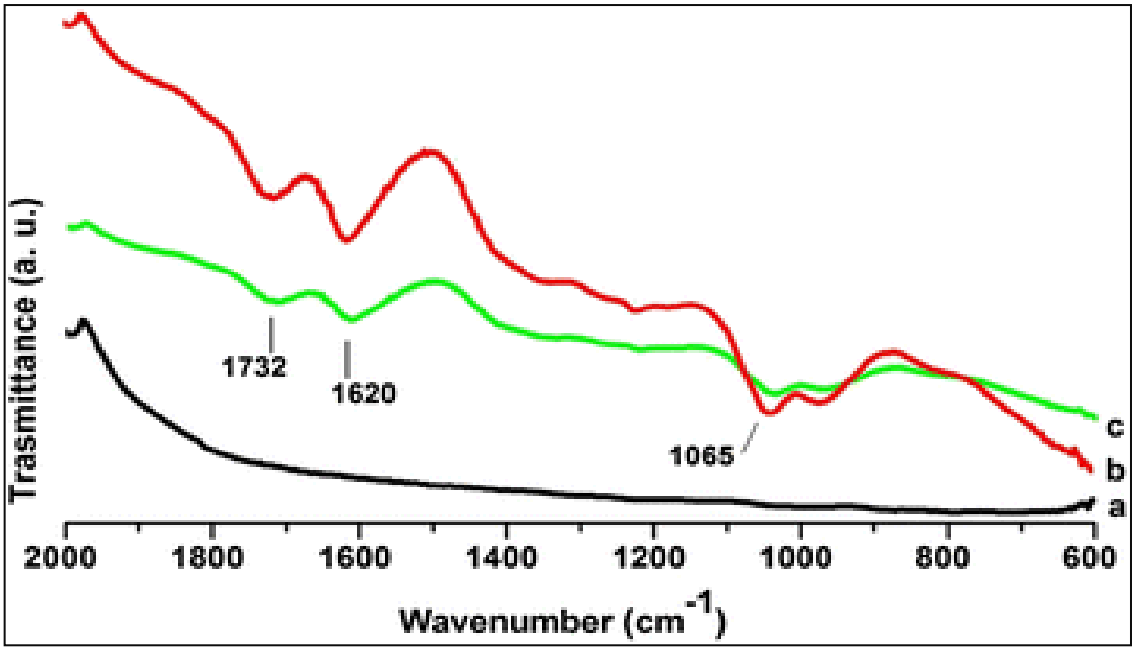

Figure 6. FTIR spectra of (a) TiO_2 (black), (b) GEO (green), (c) G-TiO2 (red) nanocomposites.

ISSN: 0976 – 2965
IJBET (2017), 6(3):18-31

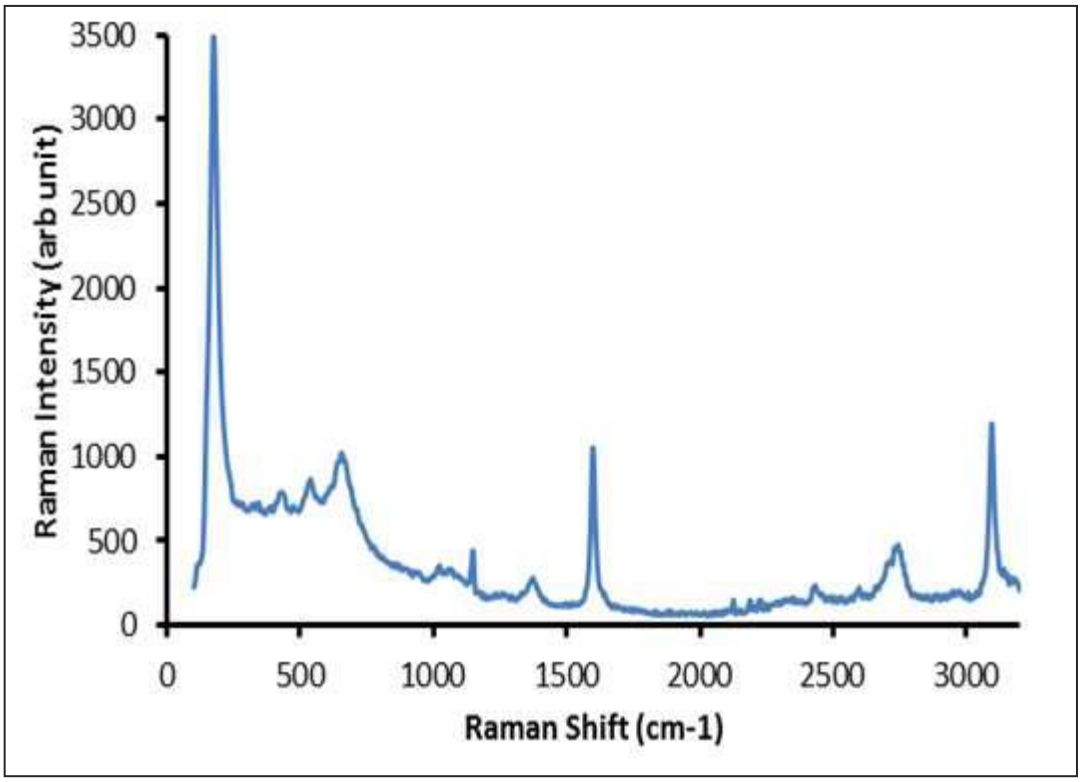

Figure 7. Raman spectra of G-TiO2 nanocomposite.

ISSN: 0976 – 2965
IJBET (2017), 6(3):18-31

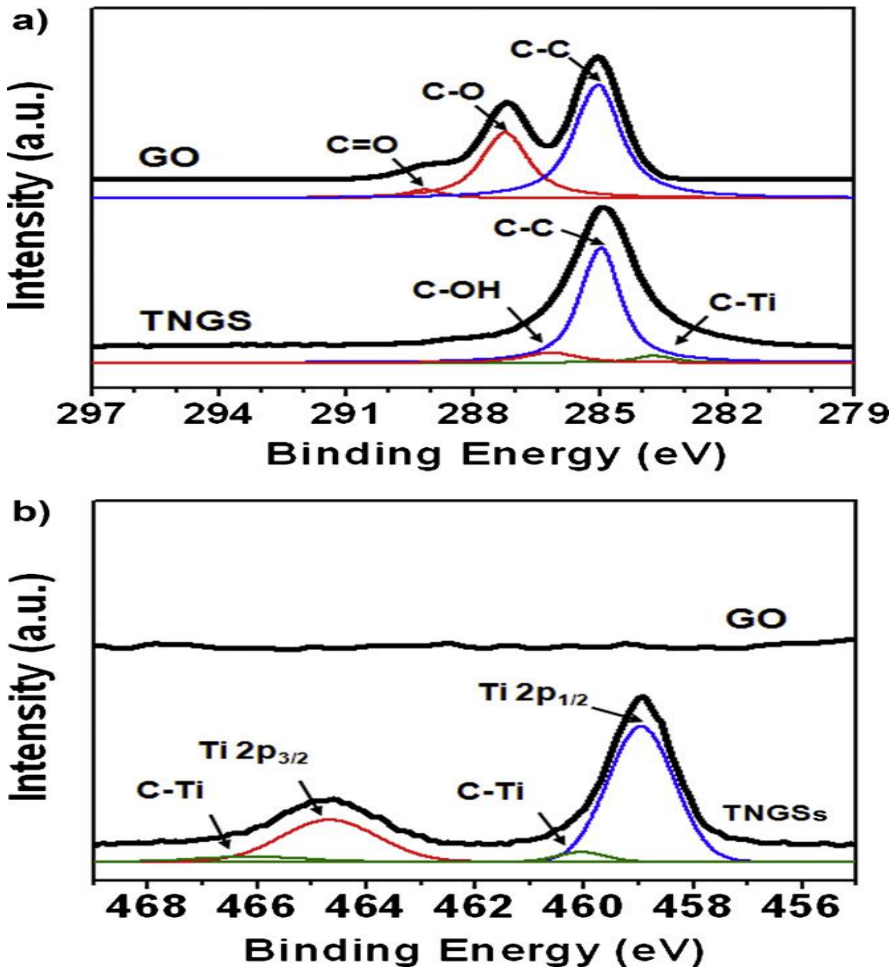

Figurer 8. XPS peak deconvolution of graphene oxide (GO) and TNGSs at (a) the C1s core level and (b) at the Ti2p core level.

ISSN: 0976 – 2965
IJBET (2017), 6(3):18-31

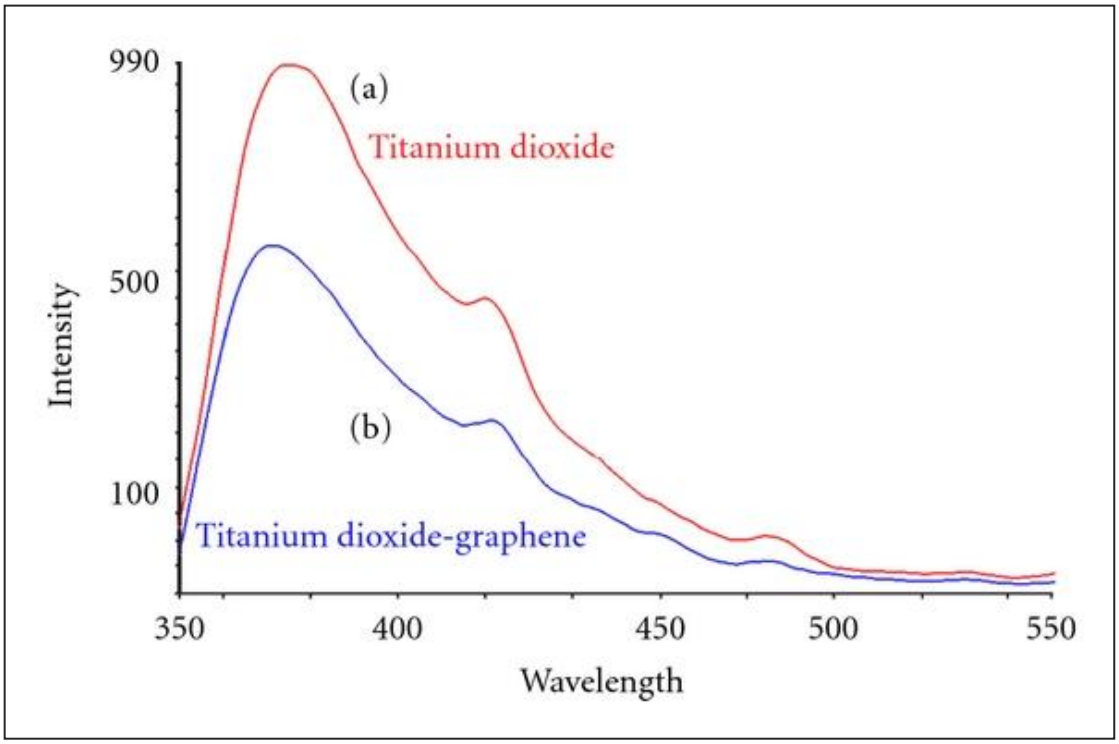

Figure 9: Fluorescence emission spectra of (a) TiO_2 and (b) TiO_2-GEO.

Table 1. The compared remediation of organic pollutants with GEO-TiO_2 nanocomposite without surfactant in the visible light.

Material/Method	Pollutant	Results[a]± S.D.
GEO-TiO_2 nanocomposite	2, 4-dihydroxybenzoic acid	96% ±0.107 in 4 h
GEO-TiO_2 nanocomposite	4-chlorophenol	94% ±0.165 in 4 h
GEO-TiO_2 nanocomposite	Toluene	90% ±0.117 in 4 h
GEO-TiO_2 nanocomposite	naphthalene	41% ±0.123 in 4 h

a: Mean of five determinations

Table 2. The compared remediation of organic pollutants with GEO-TiO_2 nanocomposite with surfactant in the visible light.

Material/Method	Pollutant	Results[a]± S.D.
GEO-TiO_2 nanocomposite	2, 4-dihydroxybenzoic acid	98% ±0.096 in 4 h
GEO-TiO_2 nanocomposite	4-chlorophenol	95% ±0.104 in 4 h
GEO-TiO_2 nanocomposite	Toluene	92% ±0.158 in 4 h
GEO-TiO_2 nanocomposite	naphthalene	55% ±0.100 in 4 h

a: Mean of five determinations

ISSN: 0976 – 2965
IJBET (2017), 6(3):18-31

Table 3. The compared remediation of organic pollutants with GEO-TiO_2 nanocomposite with surfactant in the UV light.

Material/Method	Pollutant	Results[a] ± S.D.
GEO-TiO_2 nanocomposite	2, 4-dihydroxybenzoic acid	99.5% ±0.162 in 4 h
GEO-TiO_2 nanocomposite	4-chlorophenol	98.5% ±0.162 in 4 h
GEO-TiO_2 nanocomposite	Toluene	98% ±0.162 in 4 h
GEO-TiO_2 nanocomposite	naphthalene	95% ±0.162 in 4 h

a: Mean of five determinations

X-Ray Diffraction (XRD)

XRD analysis on GEO-TiO_2 is as shown in Figure 3. The strong diffraction peak at 26.51 is indicative of presence of graphene oxide in GEO-TiO_2 structure. The presence of peaks at 25.27, 37.85, 47.83, 54.55, 63.59, 70.15, 83.1 degrees are due to TiO_2 anatase phase present in GEO-TiO_2 nanocomposite. The structure indicates the formation of crystallinity in GEO-TiO_2 nanocomposite.

Particle Analyzer

It is important to test GEO-TiO_2 particle size distribution in water. To determine such behavior, GEO-TiO_2 particles were dispersed in water. Figure 4 displays the agglomeration of nanocomposite in contaminated water, and indicating the distribution of particles. The nanocomposite particles in water form aggregation, and it shows agglomeration up-to µm in size. The small aggregation of 100 nm is also observed in Figure 4, it shows prominent 100 nm to 1 µm particle size distribution of GEO-TiO_2 in water samples. The specific surface area of the prepared TiO_2-GEO nanocomposites calculated by the multi-point Brunauer-Emmett-Teller (BET) method and total pore volume are examined. According to IUPAC notation [22], microporous and macroporous materials have pore diameters smaller than 2 and greater than 50 nm, respectively; the mesoporous category thus lies in the middle. As for all the GEO-TiO_2 nanocomposites, there is an agreement with the De Boer classification attributed to mesoporous solids [23]. The maximum of average pore size lies between 20 and 35 nm and all prepared TiO_2-GEO nanocomposites particles have mesoporous texture. It was observed that with increasing content of GEO in the composite decreasing trend of specific surface area. This may be attributed to agglomeration GEO, which occurs at higher concentrations. Graphene oxide nanosheets are covered with TiO_2 nanoparticles. Therefore when the surface area of TiO_2-GEO nanocomposites was measured, its size is dominantly determined by surface properties of anatase nanoparticles. For this reason, relatively low specific surface of the TiO_2-GEO nanocomposites (200 m2g-1) was found compared to the theoretical value of the graphene oxide. Nevertheless mesoporous TiO_2-graphene oxide nanocomposites have specific surface area in interval ~ 80–200m^2g^{-1} being considerably larger than those of GEO and relatively close to the prepared TiO_2 particles without using GEO.

UV-Visible Spectroscopy

Figure 5 shows UV-visible absorption spectrum of TiO_2 (blue) and GEO-TiO_2 nanocomposite material (red). The results has shown strong absorption band from 250 to 400 nm due to doping of graphen-oxide onto TiO_2 particles, the absorption spectra strongly continues till 570 nm, suggesting that GEO-TiO_2 nanocomposite functions effectively in both UV and visible spectrum of light. The band gap of TiO_2 nanopartciles are estimated to be 3.2 eV. It can be seen that there is a red shift of band edge and reduction of band gap to 2.7 eV is due to graphene oxide doping. The shift for the GEO-TiO2 nanocomposite towards the visible range and enhanced absorption indicates the presence of graphene oxide. This is may be an indication that GEO-TiO_2 can work well better than TiO2 for photocatalysis but under visible range.

FTIR analyses Spectroscopy

FTIR analyses were performed in order to investigate the inter-action between TiO_2 and GEO. As shown in Figure 6 the IR spectrum of TiO_2 shows

a broad band at 3400 cm−1 and the band at 1625 cm−1 originates from the surface-adsorbed water, and this indicates the presence of −OH groups on the surface of TiO_2. Comparatively, the band at 2400–3400 cm−1 of TiO_2-grapheneoxide is broader, thus indicating the presence of hydrogen bonding in the synthesized composite. TiO_2 spectrum displays three characteristic peaks at 3370, 1630 and 650 cm^{-1} associated with stretching vibrations of hydrogen-bonded water molecules and hydroxyl groups bending vibrations of OH group and Ti-O-Ti bridging stretching mode respectively. In the FTIR spectrum of GEO-TiO_2 three new features appeared. A small shoulder at 2900 $cm^{-1}$is assigned to C- H stretching in GEO and a peak at 1170 $cm^{-1}$is associated with C-O stretching vibration. It was also observed that the broad absorption below 1000 cm^{-1} became wider and shifted toward high wave number when compared to that of TiO_2. This behaviour was associated to a combination of Ti-O-Ti and Ti-O-C vibrations and suggests that the coupling between TiO_2 and GEO is achieved by the formation of the Ti-O- C bond. Since hydrazine reduction introduces nitrogen groups onto graphene, the OH groups present on the surface of TiO_2 could form hydrogen bonds with the NH groups present on the graphene sheets of the composite. In addition, a new band at 1210 cm^{-1} is observed in the spectrum obtained for TiO_2-GEO, and this can be assigned to Ti–O–C vibrations. Since hydrazine does not cause a full reduction of graphene oxide, the Ti–O–C bond may be formed when OH groups present in TiO_2 react with residual OH groups present on the graphene oxide sheets.

Raman analyses Spectroscopy

From figure 7, it has been observed that there are four peaks at low frequency region. They are assigned to the E1g (176cm-1), B1g (446cm-1), A1g (552 cm-1) and Eg (672cm-1) modes of anastase phane respectively. Like typical of graphene, D30 peak, G-peak and 2d-peak has been seen at 1390 cm^{-1}, 1600 cm^{-1} and 2750 cm^{-1}
respectively.

Binding energy analyses

X--ray photoelectron spectroscopy (XPS) was utilized to investigate the reduction of GEO as well as the hybridization of graphene and TiO_2 nanocomposite (Figure 8 a, b). The characteristic peaks of GEO in the deconvoluted C1s region appeared at 285.0, 286.1, and 289.2 eV, which were assigned to the C-C, C-O, and C= O functional groups, respectively. In contrast, in the case of the GEO-TiO_2, low-intensity oxygen peaks were confirmed, indicating a higher degree of reduction. Moreover, the band at 283.7 eV was assigned to the presence of the Ti-C bond. In the case of the Ti2p XPS spectra in Figure 8b, two bands were located at binding energies of 464.5 and 458.9 eV, which were assigned to Ti2p1/2 and Ti2p3/2, respectively. The peak deconvolution of the Ti2p spectrum confirmed two low-intensity peaks centered at 465.8 and 460.2 eV, which were assigned to the Ti–C bond. On the basis of these results, one may conclude that TiO_2 particles chemically anchored onto grapheme oxide sheets were prepared successfully through the non-hydrolytic sol–gel reaction.

Fluorescence Emission Spectroscopy

It is well known that photocatalytic activity is a function of lifetime of trapping electron and hole pairs, recombination of electron and hole pairs can emit energy in the form of fluorescence. Fluorescence emission spectra are a useful characterization technique to investigate the efficiency of charge carrier trapping and to understand the fate of e−/h+ pairs in semiconductor particles like TiO_2. Recombination of electron and hole pairs can emit energy in the form of fluorescence as seen from Figure 9, the fluorescence intensity of TiO_2-GEO is lower than that of TiO_2. This indicates that the recombination of electron and hole pairs is suppressed in the presence of graphene oxide, which possibly indicates an increase in photocatalytic efficiency. In addition, the fluorescence emission spectra displayed 3 main peaks at 380 nm, 420 nm, and 484 nm for both TiO_2 and TiO_2-GEO, which are attributed to the self-trapped excitons localized on TiO_6 octahedra and oxygen vacancies. Thus, this indicates that the presence of graphene does not alter the mechanism of TiO_2 photocatalysis.

Photoelectrochemical degradation activities of TiO2-GEO.

Four organic pollutants were chosen as the model organic pollutant to evaluate the photoelectrochemical degradation activities of the prepared TiO_2-GEO nanocomposite. The concentration of pollutants were monitored by measuring the absorbance at a wavelength characteristic of each one. The suspension composed of TiO_2-GEO were stirred in the dark for

about 30 min to achieve absorption-desorption equilibrium. Apparent degradation of organic pollutants was observed as soon as the Photoelectrochemical degradation activities of TiO2-GEO reaction was initiated by introducing illumination as well as H_2O_2 to the system. It can be observed that the degradation accelerated as the amount of the catalyst increased from 0.1 to 1.5 g/L. This phenomenon can be attributed to the reason that the number of the reactive sites on TiO_2-GEO surface increased when the amount of catalyst increasing. In this study, the optimal amount of the catalyst (1.5 g/L) were used throughout our experiments. 50 ppm of organic pollutants (2, 4-dihydroxybenzoic acid, 4-chlorophenol, Toluene and naphthalene) were used in 250 ml aqueous solution, 1 g of GEO-TiO_2 nanocomposite have been used under 100 W visible light bulb. Table 1 shows 96% of 2, 4-dihydroxybenzoic acid, 94% of 4-chlorophenol, 90% of toluene, only 40% of naphthalene remediation from the contamination water for exposure of 4 hour of visible light, without using surfactant. And Table 2 shows 98% of 2, 4-dihydroxybenzoic acid, 95% of 4-chlorophenol, 92% of toluene, only 55% of naphthalene remediation from the contamination water for exposure of 4 hour of visible light, with using surfactant. Indeed, further light exposure results in similar values indicating that organic pollutants on surface of water mostly evaporated or there could be continual evaporation of organic pollutants from water surface. We have also observed that without the use of graphene oxide in TiO_2, remediation of organic pollutants in visible light excitation were poor. Naphthalene is sparingly soluble in water so we used surfactants in naphthalene solution, as well as in other organic pollutants . After using the surfactant, the decontamination of naphthalene under visible light in presence of GEO-TiO_2 nano-composite particles was 55% over a period of 4 h, measured using HPLC. Moreover, the decomposition of of naphthalene after using the surfactant, under UV light in presence of GEO-TiO_2 nano-composite particles was 95% over a period of 4 h. Indeed, the results have shown that is difficult to decontaminate naphthalene under visible light. So, organic pollutants with low solubility in aqueous solution are not in contact with GEO-TiO_2 nanocomposite unless surfactant is added, does not display satisfactory reduction after 48 h of visible light irradiation. The results in Table 3 shows that 99.5% of 2, 4-dihydroxybenzoic acid, 98.8% of 4-chlorophenol, 98.5% of toluene, 96% of naphthalene have been remediated using GEO-TiO_2 nanomaterial under UV light. The insolubility of organic pollutants in water brings contaminant to the surface of water thereby inhibiting photocatalytic effect with G-TiO_2. However, when the contaminants soluble in water increase, they remain in contact with GEO-TiO_2 surface particles and are completely remediated. Thus, it is advisable to add surfactant (such as dodecyl sulphonate) inorder to increase the solubility of organic contaminants in aqueous solution, which helps contaminant to remain adsorped to the TiO_2-GEO nanocomposites surface, this may be due to π-π conjugation accumulation effect between TiO_2-GEO and organic pollutants. The results suggesting the importance of organic pollutant to come in contact with photocatalyst surface for complete remediation.

CONCLUSION

Based on the results shown in this research, it can be concluded that TiO_2-GEO nanocomposite material have outstanding properties in the design of high-performance photocatalysts that might be integrated in diverse applications as water/wastewater treatment. The present work overviews some important aspects of graphene oxide-TiO_2 photocatalysts, such as methods of synthesis, associated photocatalytic mechanisms and applications for the photocatalytic degradation of organic pollutants. GEO-TiO_2 nanocomposites were synthesized using sol-gel technique, the liquid phase deposition method and their catalytic activity was measured. Finally, the immobilization of GEO-TiO_2 nanocomposite material with sufficient capacity to degrade water pollutant. This fact promises a new trend in the application of carbon nanomaterials without doping as photocatalysts. Visible light decomposition mineralization measured by COD indicates that up to 98% of organic matter is removed through photocatalysis using GEO-TiO_2. In addition, research findings show that nanometric size plays an important role in photocatalytic processes, reflected in the fact that GEO show better results in eliminating pollutants than TiO_2 alone. Thus, it can be concluded that, photocatalysis with GEO-TiO_2 is simple and effective, because, avoids the use of any oxidizing agent. And thereby a new line of research in photocatalysis with GEO-TiO_2 nanomaterials focused in the treatment of contaminated water, depending on the structural features of these materials, their electronic properties, dimensions

and functional groups in the nanocomposite surface.

REFERENCES

[1] Daghrir R., Drogui P., Robert D. (2013) Modified TiO_2 for environmental photocatalytic applications: a review. Ind. Eng. Chem. Res., 52 (10): 3581–3599.

[2] Anil Kumar Reddy P., Venkata Laxma Reddy P., Maitrey Sharma V., Srinivas B., Kumari V.D., Subrahmanyam M. (2010) Photocatalytic degradation of isoproturon pesticide on C, N and S doped TiO2. J. Water Resour. Prot., 02: 235–244.

[3] Akpan U.G., Hameed B.H. (2009) Parameters affecting the photocatalytic degradation of dyes using TiO2-based photocatalysts: a review. J. Hazard. Mater., 170: 520–529.

[4] Gupta S.M., Tripathi M. (2011) An overview of commonly used semiconductor nanoparticles in photocatalysis. High Energy Chem., 11: 46, 1–9.

[5] Xia F., Mueller T., Lin Y.M., Valdes-Garcia A., Avouris P. (2009) Ultrafast grapheme photodetector. Nat. Nanotechnol, 4: 839–843.

[6] Oliveira A.S., Saggioro E.M., Pavesi T., Moreira J.C., Filipe L., Ferreira V. (2016) Solar Photochemistry for Environmental Remediation—Advanced Oxidation Processes for Industrial Wastewater Treatment; In. Tech: Lisboa, Portugal.

[7] Morales-Torres S., Pastrana-Martínez L.M., Figueiredo J.L., Faria J.L., Silva A.M.T. (2012) Design of graphene-based TiO2 photocatalysts—A review. Environ. Sci. Pollut. Res. Int., 19: 3676–3687.

[8] Chand R., Obuchi E., Katoh K., Luitel H.N., Nakano K. (2013) Effect of transition metal doping under reducing calcinations atmosphere on photocatalytic property of TiO2 immobilized on SiO2 beads. J. Environ. Sci., 25: 1419–1423.

[9] Brownson D.A.C., Kampouris D.K., Banks C.E. (2011) An overview of graphene in energyproduction and storage applications. J. Power Sourc., 196: 4873–4885.

[10] Wan-Kuen R. et al. (2016) Cobalt promoted TiO_2/GO for the photocatalytic degradation of oxytetracycline and Congo Red. Applied Catalysis B: Environmental, 201: 159–168.

[11] Fujishima A., Honda K. (1972) Photolysis-decomposition of water at the surface of an irradiated semiconductor. Nature, 238: 37–38.

[12] Yang H. G. et al. (2008) Anatase TiO2 single crystals with a large percentage of reactive facets. Nature, 453: 638–641.

[13] Crossland E. J. W. et al. (2013) Mesoporous TiO_2 single crystals delivering enhanced mobility and optoelectronic device performance. Nature, 495: 215–219.

[14] Chen X., Liu L., Yu P. Y., Mao S. S. (2011)Increasing Solar Absorption for Photocatalysis with Black Hydrogenated Titanium Dioxide Nanocrystals. Science, 331: 746–750.

[15] Qiu B., Xing M., Zhang J. (2014) Mesoporous TiO_2 Nanocrystals Grown in Situ on Graphene Aerogels for High Photocatalysis and Lithium-Ion Batteries. J. Am. Chem. Soc., 136: 5852–5855.

[16] Zhang H., Lv X., Li Y., Wang Y., Li J. (2009) P25-Graphene Composite as a High Performance Photocatalyst. ACS Nano, 4: 380–386.

[17] Mo R., Lei Z., Sun K., Rooney D. (2014) Facile Synthesis of Anatase TiO2 Quantum-Dot/Graphene-Nanosheet Composites with Enhanced Electrochemical Performance for Lithium-Ion Batteries. Adv. Mater., 26: 2084–2088.

[18] Xing M., Li X., Zhang J. (2014) Synergistic effect on the visible light activity of Ti3+ doped TiO2 nanorods/boron doped graphene composite. Sci. Rep., 4: 5493–5499.

[19] Xiangang H., Li M., Jianping W., Qixing Z. (2012) Covalently synthesized graphene oxide-aptamer nanosheets for efficient visible-light photocatalysis of nucleic acids and proteins of viruses. Carbon, 50: 2772–81.

[20] Bustos-Ramirez K., Martinez-Hernandez A.L., Martinez-Barrera G., de Icaza-Herrera M., Castaño M.V., Velasco-Santos C. (2013) Covalently bonded chitosan on graphene oxide via redox reaction. Materials, 6: 911–26.

[21] Gunti, S., Kumar, A. and Ram, M.K. (2015) Comparative Organics Remediation Properties of Nanostructured Graphene Doped Titanium Oxide and Graphene Doped Zinc Oxide Photocatalysts. American Journal of Analytical Chemistry, 6: 708-717.

[22] Lowell S., Shields J.E. (1998) Powder Surface Area and Porosity. Google Scholar

[23] de Boer J.A. (1958) In Structure & Properties of Porous Materials. Google Scholar